Experimental observation of vortex rings in a bulk magnet

Claire Donnelly[1,2,3] ✉, Konstantin L. Metlov[4,5] ✉, Valerio Scagnoli[2,3], Manuel Guizar-Sicairos[3], Mirko Holler[3], Nicholas S. Bingham[2,3], Jörg Raabe[3], Laura J. Heyderman[2,3], Nigel R. Cooper[1] and Sebastian Gliga[3] ✉

Introduction

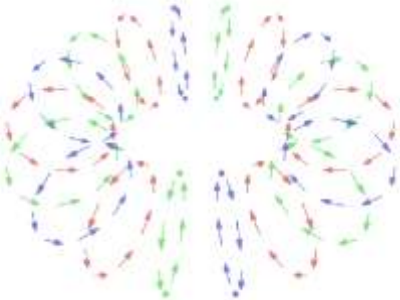

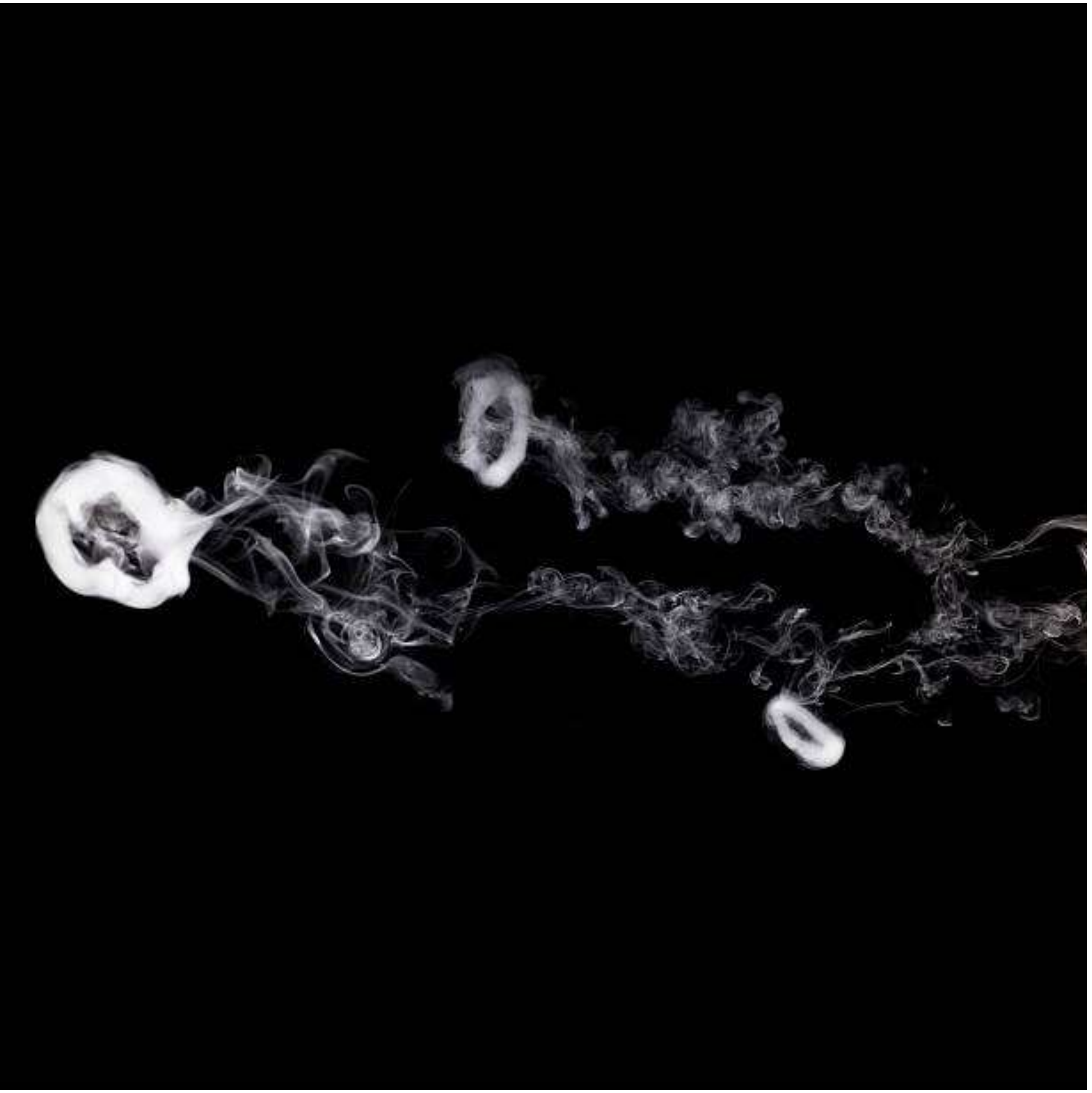

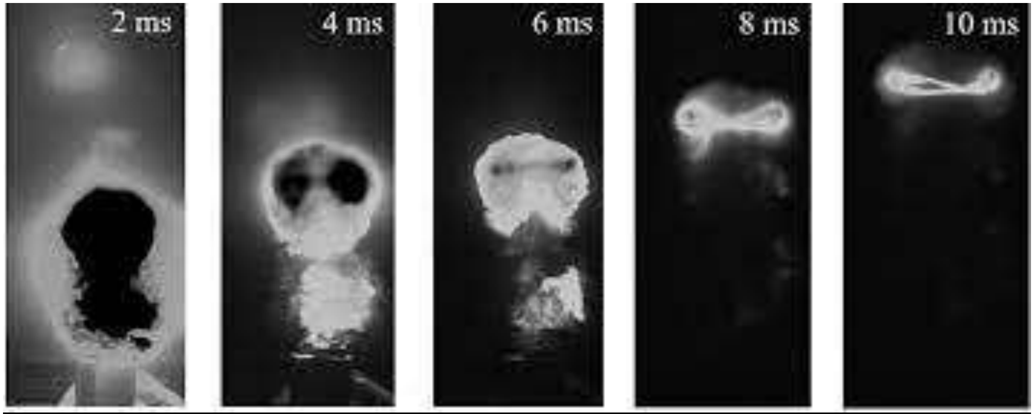

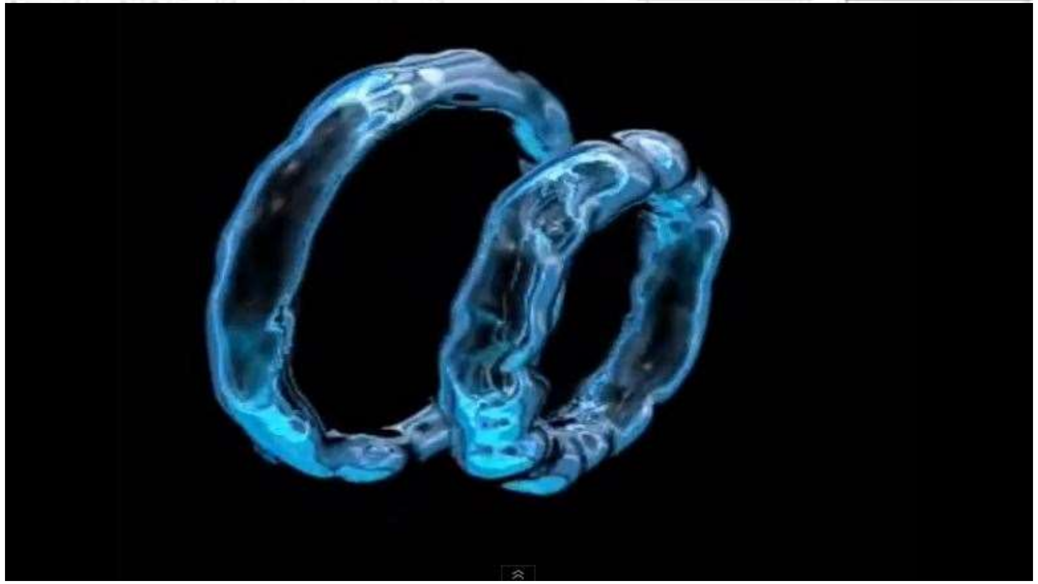

Overview

1. Vortex rings and bloch points in a bulk magnet
2. Experimental investigation and setup
3. Results
4. Outlook

Vortex rings and bloch points in a bulk magnet

Magnetic vorticity $\Omega_\alpha = \frac{1}{8\pi} \varepsilon_{\alpha\beta\gamma}\varepsilon_{ijk} m_i \partial_\beta m_j \partial_\alpha m_k$

Reduced magnetization $\mathbf{m} = \frac{M}{M_s}$

Cartesian components:

$$\begin{aligned}
\Omega_x &= 2m_x(\partial_y m_y \partial_z m_z - \partial_z m_y \partial_y m_z) + 2m_y(\partial_y m_z \partial_z m_x - \partial_z m_z \partial_y m_x) \\
&\quad + 2m_z(\partial_y m_x \partial_z m_y - \partial_z m_x \partial_y m_y) \\
\Omega_y &= 2m_x(\partial_z m_y \partial_x m_z - \partial_x m_y \partial_z m_z) + 2m_y(\partial_z m_z \partial_x m_x - \partial_x m_z \partial_z m_x) \\
&\quad + 2m_z(\partial_z m_x \partial_x m_y - \partial_x m_x \partial_z m_y) \\
\Omega_z &= 2m_x(\partial_x m_y \partial_y m_z - \partial_y m_y \partial_x m_z) + 2m_y(\partial_x m_z \partial_y m_x - \partial_y m_z \partial_x m_x) \\
&\quad + 2m_z(\partial_x m_x \partial_y m_y - \partial_y m_x \partial_x m_y)
\end{aligned}$$

In general:

$$\vec{\omega} \equiv \nabla \times \vec{u} = \epsilon_{ijk} \frac{\partial u_k}{\partial x_j}$$

with flow velocity $\vec{u}$

Here (magnetic vorticity):

$$\Omega_i \equiv \frac{1}{2} \epsilon_{ijk} \left(\partial_j \mathbf{M} \times \partial_k \mathbf{M} \right) \cdot \mathbf{M}$$

with magnetization $\mathbf{M} = \mathbf{M}(\mathbf{r}, t)$

Vortex rings and bloch points in a bulk magnet

Magnetic vorticity $\Omega_\alpha = \frac{1}{8\pi} \varepsilon_{\alpha\beta\gamma}\varepsilon_{ijk} m_i \partial_\beta m_j \partial_\alpha m_k$

Reduced magnetization $\mathbf{m} = \frac{M}{M_s}$

represents **topological charge flux density $\boldsymbol{\Omega}$**

Two dimensions	Three dimensions
Skyrmion	**Hopfion**

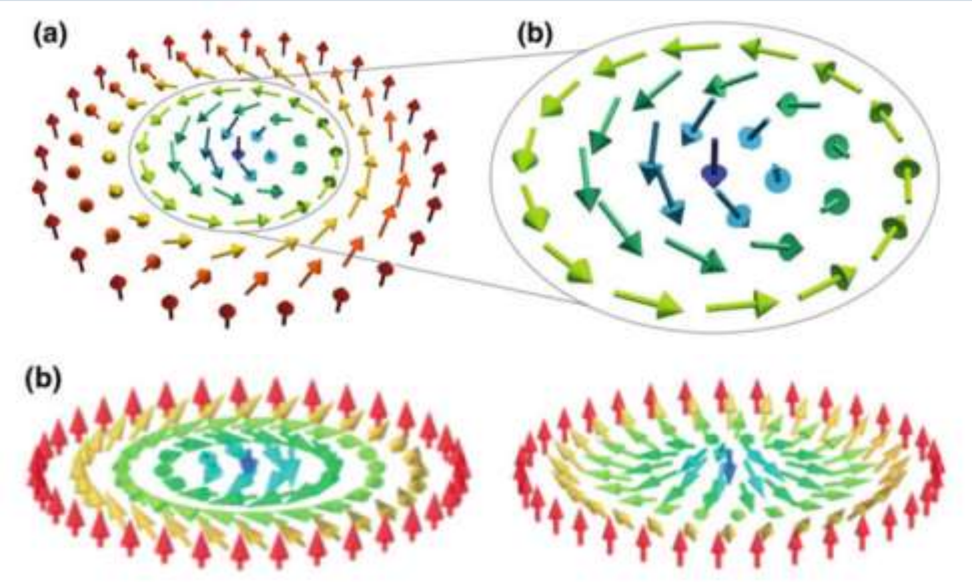

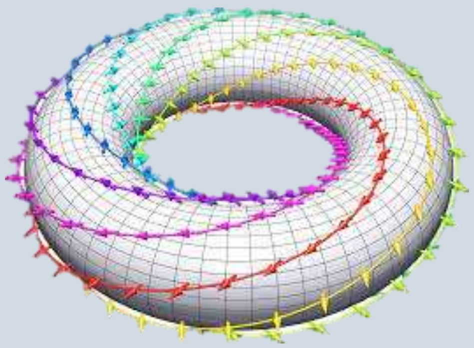

Vortex rings and bloch points in a bulk magnet

Magnetic vorticity $\Omega_\alpha = \frac{1}{8\pi}\, \varepsilon_{\alpha\beta\gamma}\varepsilon_{ijk} m_i \partial_\beta m_j \partial_\alpha m_k$

Reduced magnetization $\mathbf{m} = \frac{M}{M_s}$

represents **topological charge flux density $\boldsymbol{\Omega}$**

Vortices: naturally occuring flux closure states in which the magnetization curls around a stable core

Anti-vortices: opposite rotation of the in-plane magnetization

Vortex rings and bloch points in a bulk magnet

Magnetic vorticity $\Omega_\alpha = \frac{1}{8\pi} \varepsilon_{\alpha\beta\gamma}\varepsilon_{ijk} m_i \partial_\beta m_j \partial_\alpha m_k$

Reduced magnetization $\mathbf{m} = \frac{M}{M_s}$

Vortex **Anti-vortex**

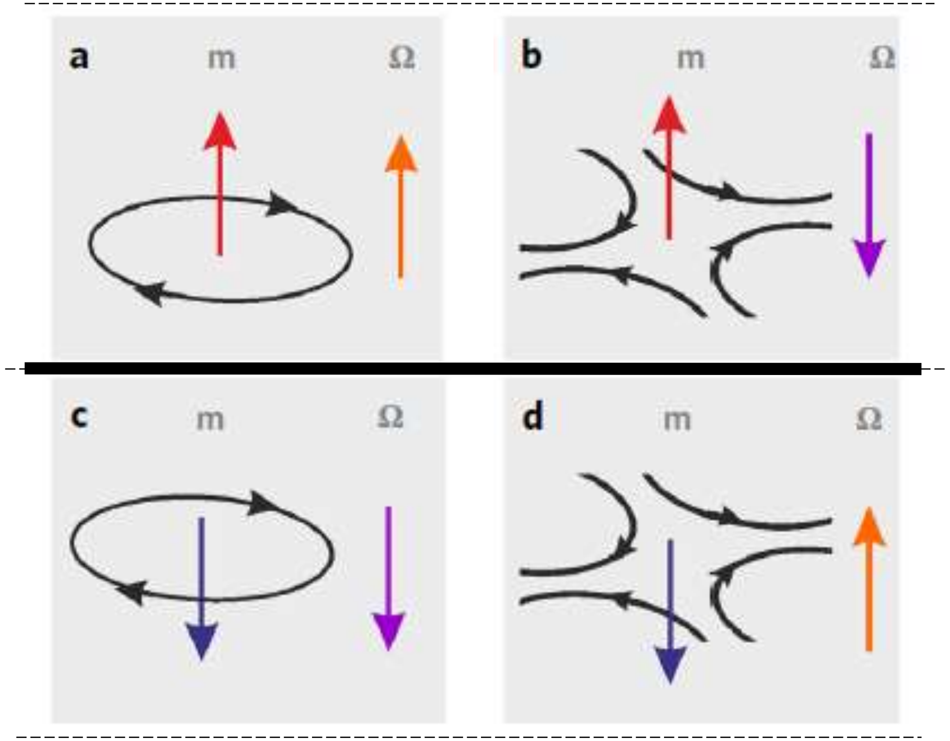

Vorticity of a ring

vortex–antivortex pair with parallel polarizations

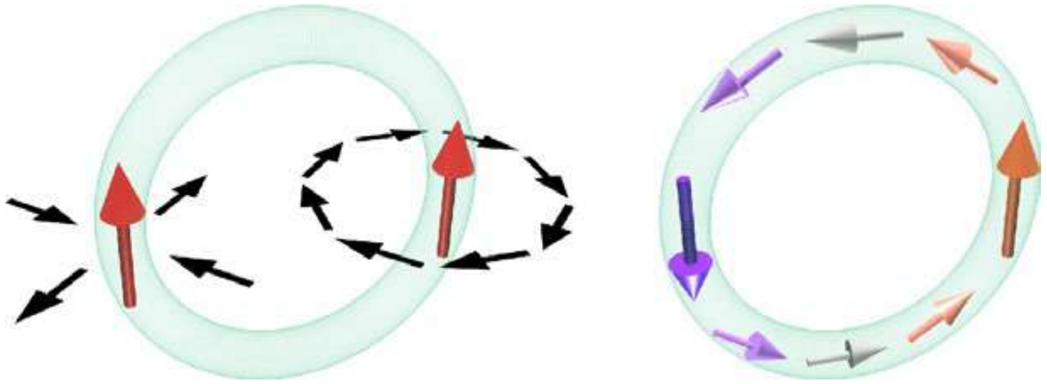

magnetization $\mathbf{m}$

Magnetic vorticity $\boldsymbol{\Omega}$

Vortex rings and bloch points in a bulk magnet

Magnetic vorticity $\Omega_\alpha = \frac{1}{8\pi}\, \varepsilon_{\alpha\beta\gamma}\varepsilon_{ijk} m_i \partial_\beta m_j \partial_\alpha m_k$

Singularities of the magnetic vorticity: $\boldsymbol{\nabla} \cdot \boldsymbol{\Omega}$

→ **Bloch points** and **anti-Bloch points**

→ Vorticity abruptly reverses sign

→Bloch point: **vorticity source**

→Anti-Bloch point: **vorticity sink**

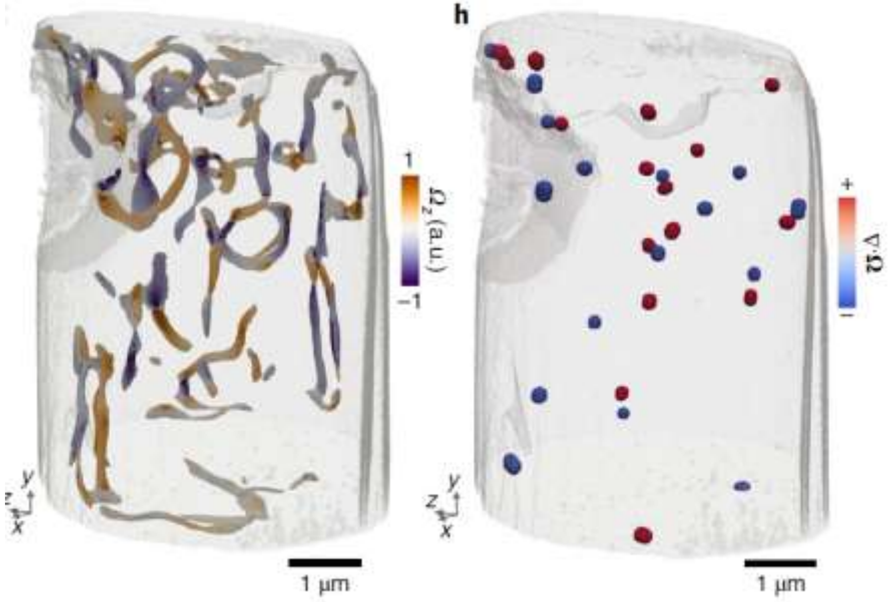

Anti-Bloch point Bloch point

Experimental Investigation

Two dimensions	Three dimensions
soft-X-ray and electron microscopies	**Hard x-ray regime**
Spatial resolution: $<$ **10 nm**	Spatial resolution: **$\sim$10 – 100 nm**
Sample thickness: $<$ **200nm and 100nm**	and Penetration depth: **Up to 10s of μm**
→ imaging is limited to **thin samples**	→ **high-spatial-resolution 3D** studies of ferromagnetic systems

Experimental Investigation

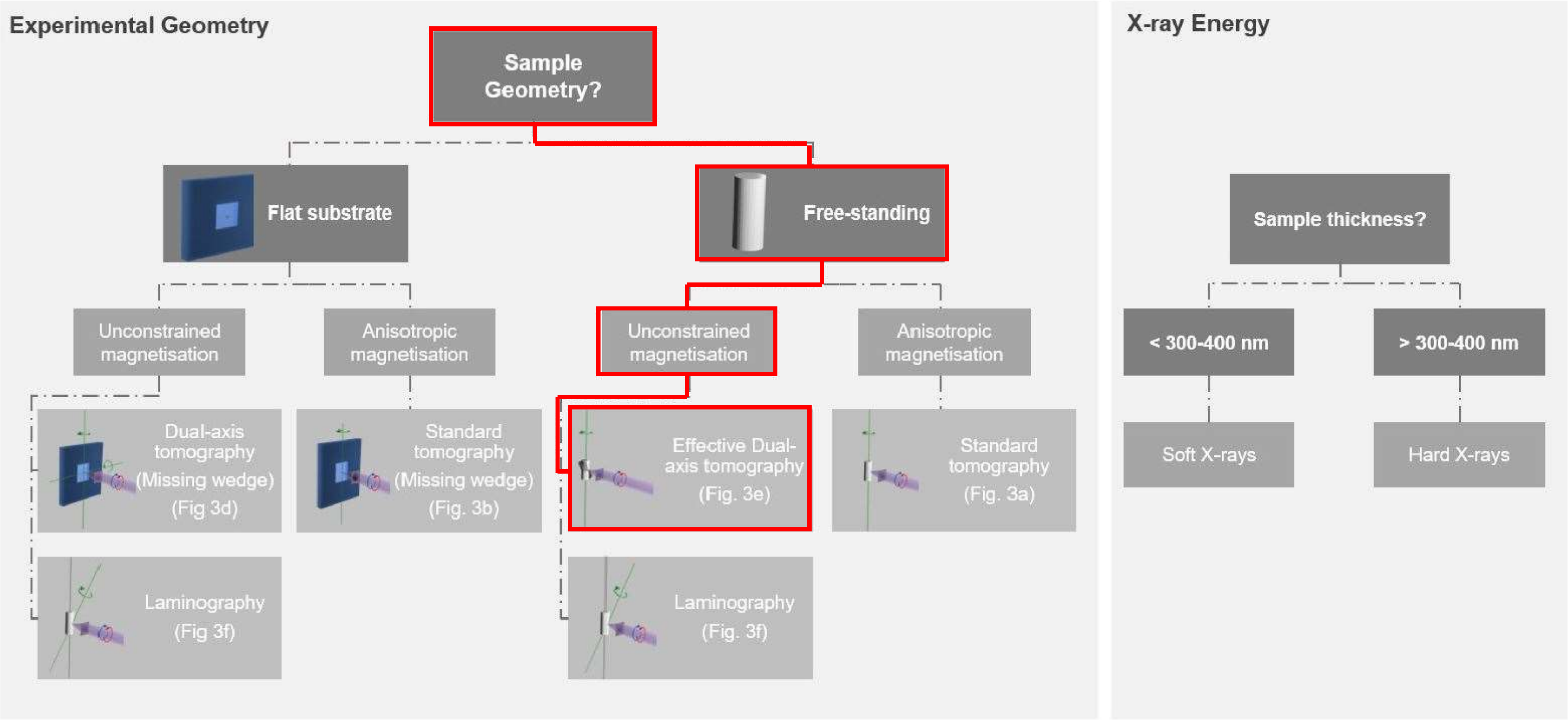

"Imaging three-dimensional magnetic systems with x-rays", C Donnelly and V Scagnoli

Experimental Investigation

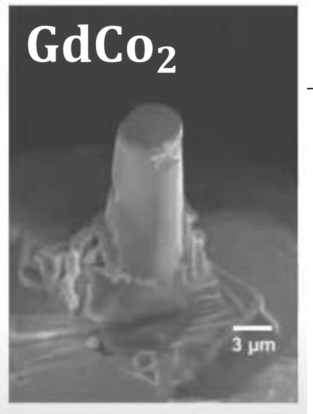

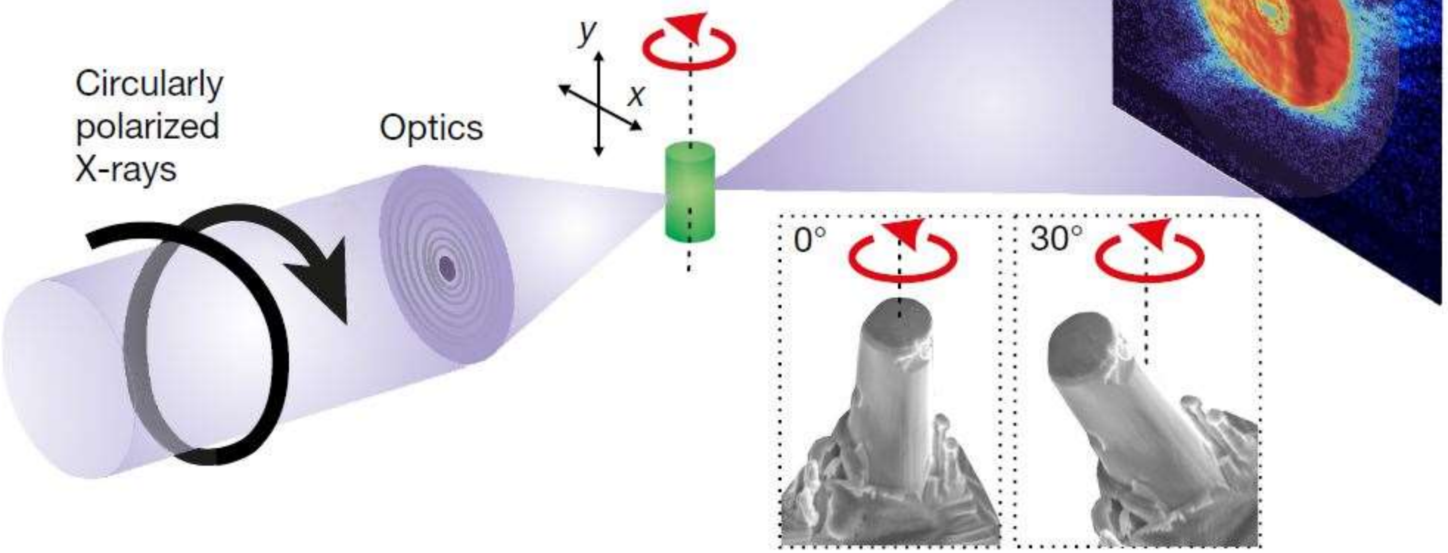

Effective dual-axis tomography

1024 different orientations distributed over **360°** with equal angular spacing

0° and 30° tilt angles

Spatial resolution:
97 nm, 125 nm and **127 nm** in the **x–z**, **x–y** and **y–z** planes

X-ray magnetic circular dichroism **(XMCD)**

Experimental Investigation

dichroism ≙ dependence of the absorption on its polarisation

X-ray magnetic circular dichroism (XMCD)

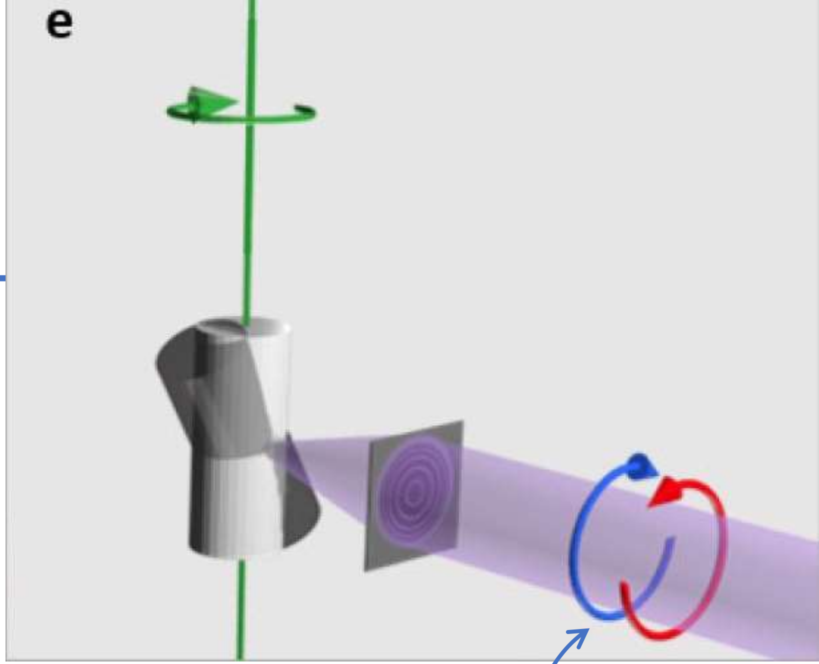

single X-ray polarization
→ only left circulary polarization

Signal takes **maximum positive** (negative) value when:

magnetic moment **parallel** (antiparallel) to x-ray propagation direction

Signal is **zero** when:

Magnetic moment **perpendicular** to X-ray propagation direction

→ upon 180° the XMCD signal is reversed in sign

Experimental Investigation

Dichroic ptychography

Ptychography ≙ coherent diffraction imaging (CDI) technique providing complex magnetic signal

Scattering factor:

$$f = \underbrace{f_c(\epsilon_f^* \cdot \epsilon_i)}_{\text{charge}} \; - \; \underbrace{i f_m^{(1)}(\epsilon_f^* \times \epsilon_i) \cdot m(r)}_{\text{circular dichroism}} \; + \; \underbrace{f_m^{(2)}(\epsilon_f^* \cdot m(r))(\epsilon_i \cdot m(r))}_{\text{linear dichroic scattering factor } f_m^{(2)} \to 0}$$

$$f = f_c - i f_m^{(1)} \begin{pmatrix} i m_z & 0 \\ 0 & -i m_z \end{pmatrix} = f_c \pm i f_m \, \hat{\mathbf{z}} \cdot \mathbf{m}(\mathbf{r})$$

ϵ_i: Jones polatization vector **incomming** wave

ϵ_f: Jones polatization vector **scattered** wave

f_c: complex valued **charge** scattering factor

$f_m^{(1)}$: complex valued **circular** dichroic magnetic scattering factor

$f_m^{(2)}$: complex valued **linear** dichroic magnetic scattering factor

Experimental Investigation

Dichroic ptychography

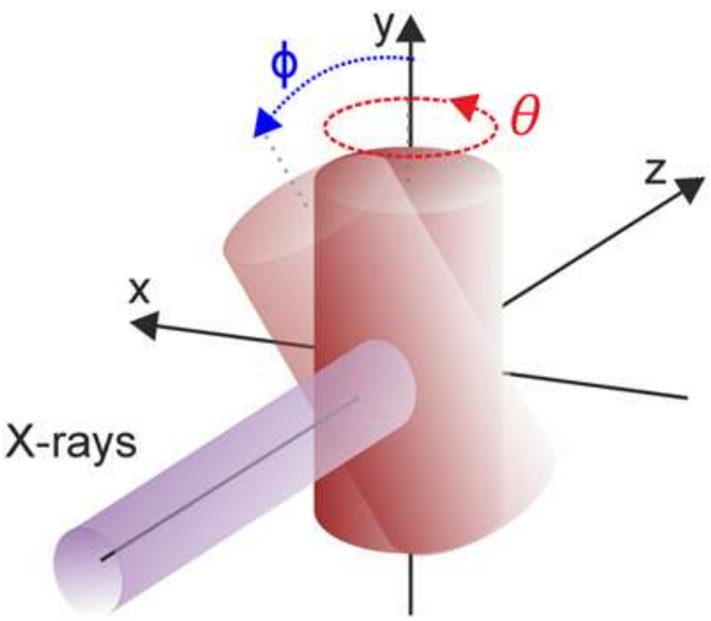

→ projections are measured at **θ and θ + 180°** using **circular left** polarization through **360°** about rotation axis

→ XMCD signal has reversed sign

→ magnetic contrast is separated from electronic contrast

→Tilted by angle **φ** (0° and 30°) to probe components of magnetization in multiple planes

➡ all components of the magnetization vector

Experimental Investigation

Dichroic ptychography

Probe and object are complex functions that interact via scalar product:

Exit field after sample $\boldsymbol{\psi_j(r) = P(r) \cdot O(r - r_j)}$

scattering factor

$\mathbf{P(r)}$: incident illumination

X-rays

Transmissivity of sample: $O(r - r_j) = \exp[\ i\frac{\omega}{c}\int\left(1 - \frac{r_{electron}}{2\pi}\lambda^2 n_{at}\, \mathbf{f(r - r_j)}\right)dz\ ]$

X-rays

→ **phase** $\boldsymbol{\phi_{XMCD}}$ and **absorption** $\boldsymbol{A_{XMCD}}$

magnetic contrast of XMCD signals

→Maximum of absorption signal at $\mathbf{E_{Photon} = 7.246\ keV}$

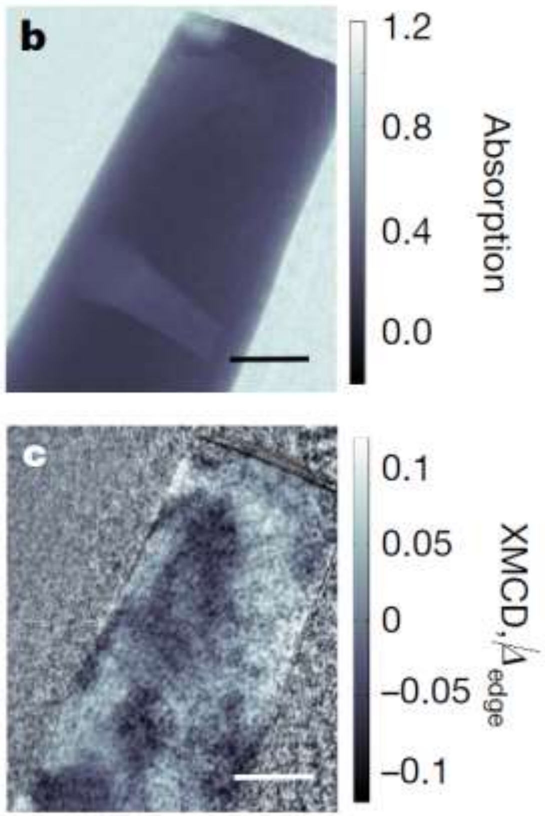

Experimental Investigation

Effective dual-axis tomography

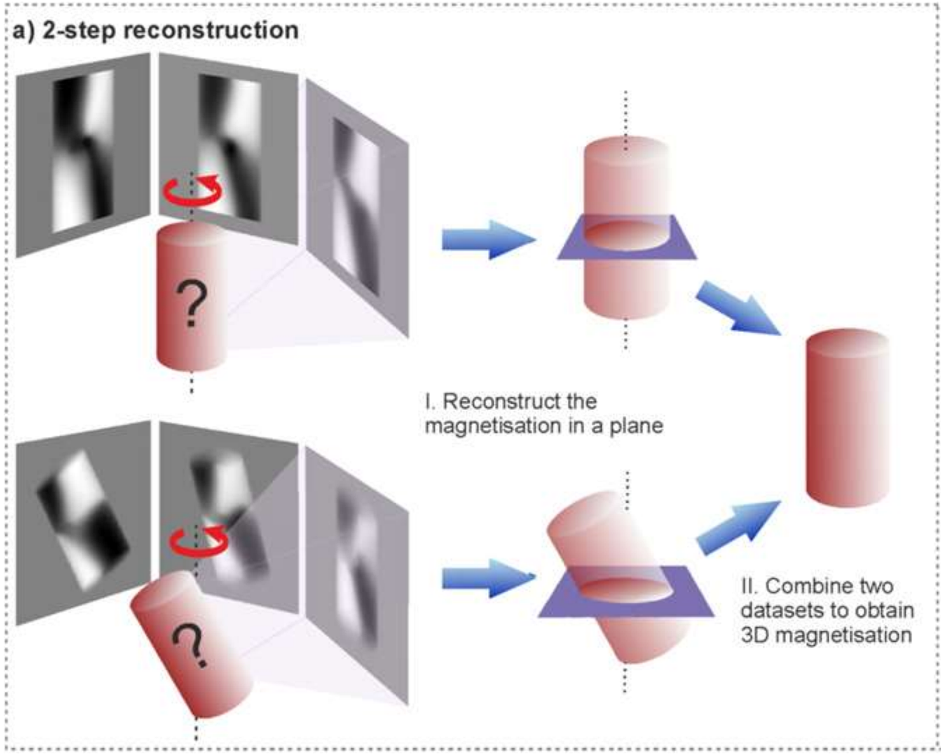

The magnetization reconstructed using

two-step gradient-based iterative reconstruction algorithm

1. Magnetization in two planes perpendicular to the axis of rotation
2. 3D magnetization determined from two components of the magnetization in each plane

Results

Axial tomographic slice

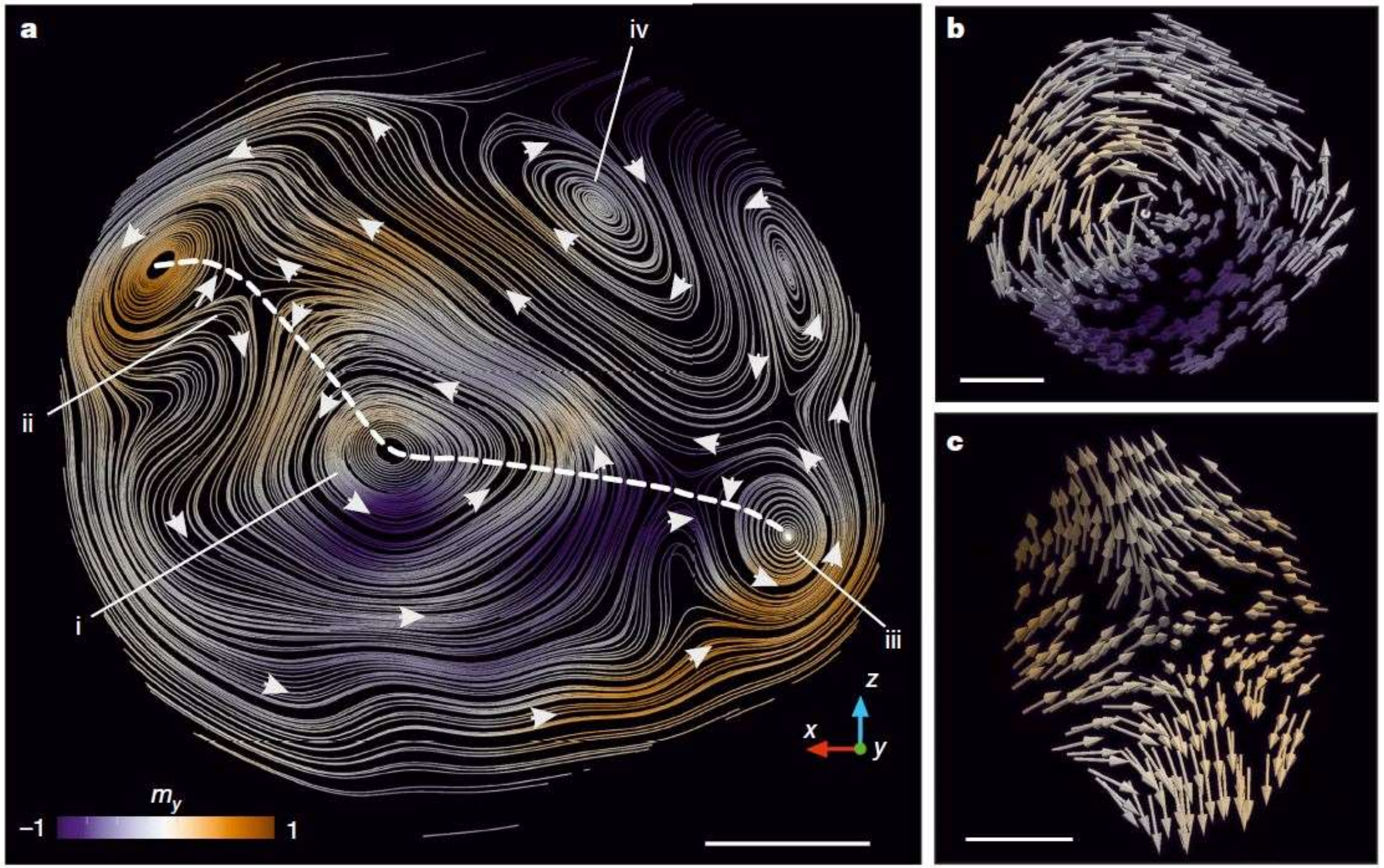

Vortex

Anti-vortex

Results

Correspondence with 3D

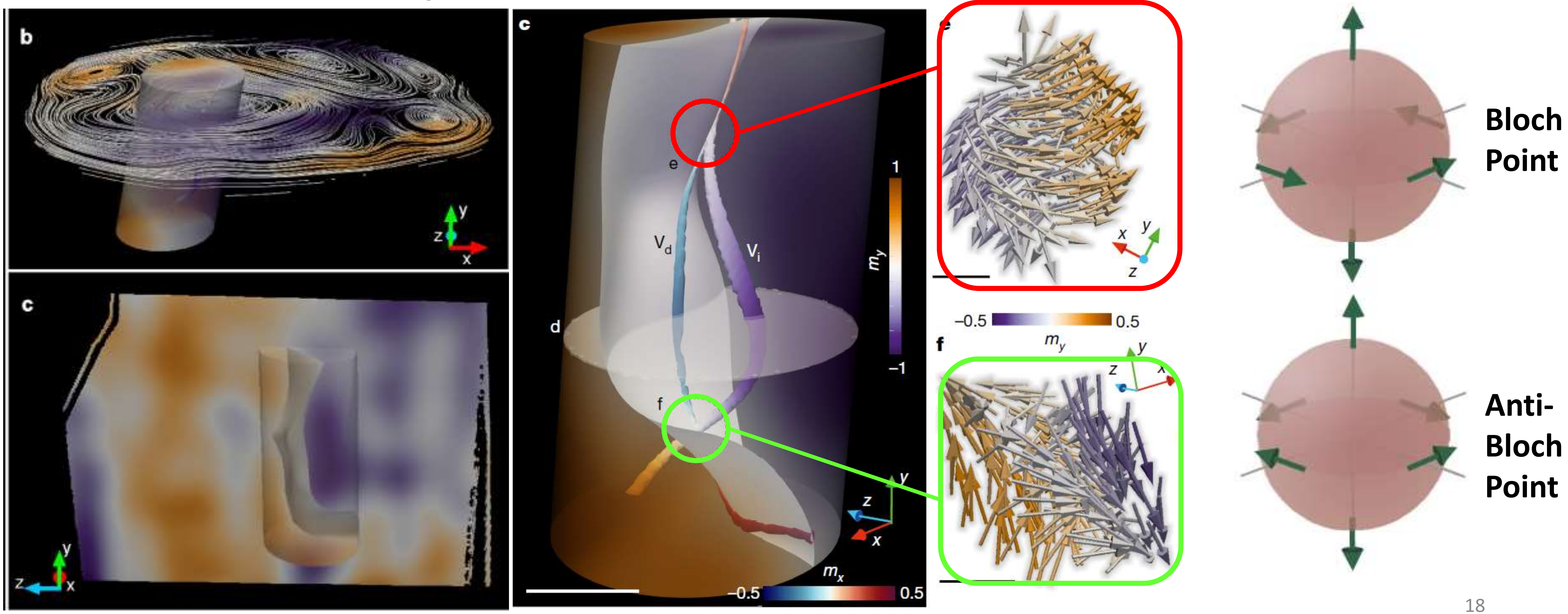

Results – simple structures and pre-images

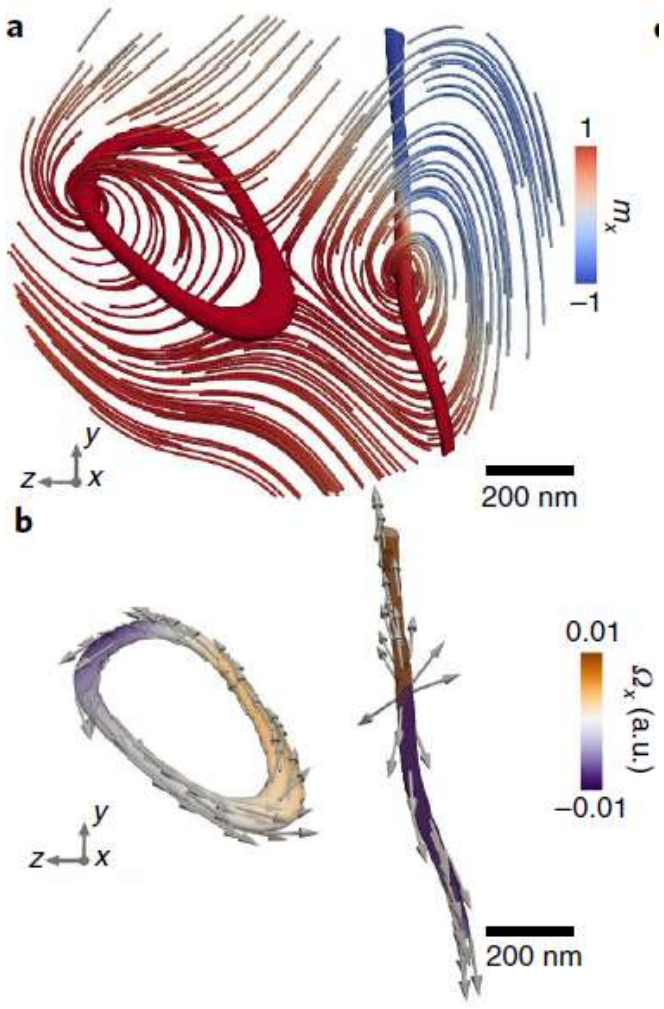

- **static** and **stable** loops at room temperature

- average diameter of the vortex rings ≈ $(\mathbf{400 \pm 90})\ \mathbf{nm}$ (y-z)-plane

- **Hopf index H = 0** → vortex rings belong to a class of non-topological solitons

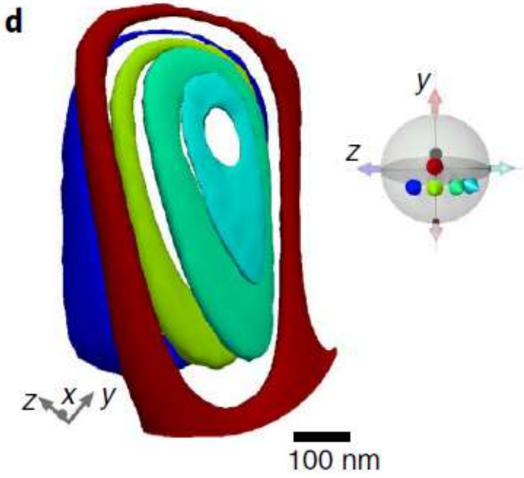

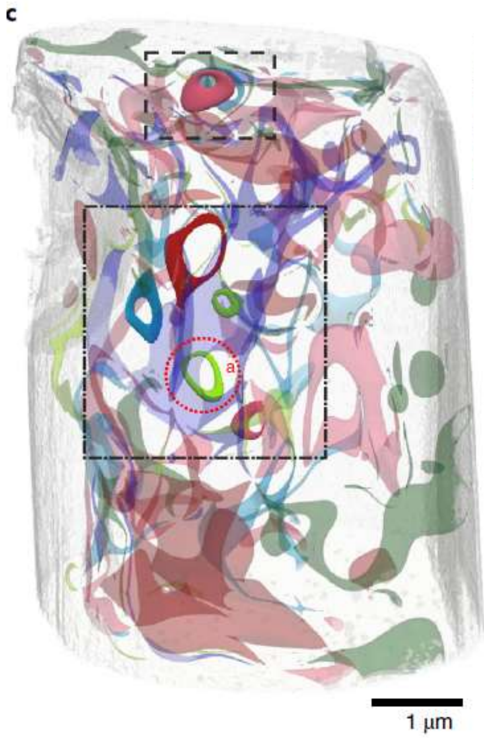

Results – Pre-images

Vortex ring:
→ vortex-antivortex pair
→ no Bloch points

Vortex loop:
→ containing **sources** and **sinks** of the magnetization due to the presence of **Bloch points**

magnetization

pre-image

vorticity distributio n

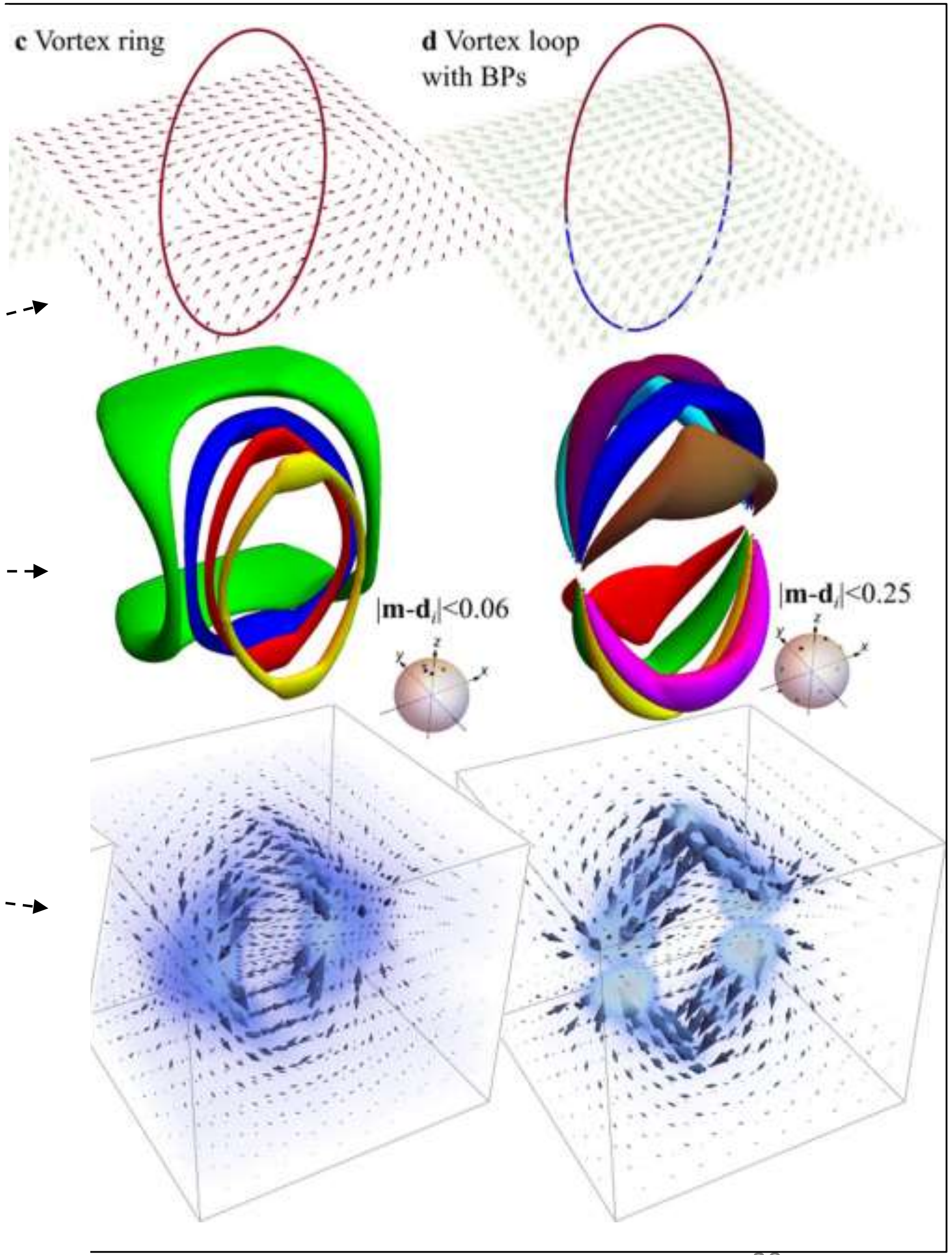

Results – vortex loops

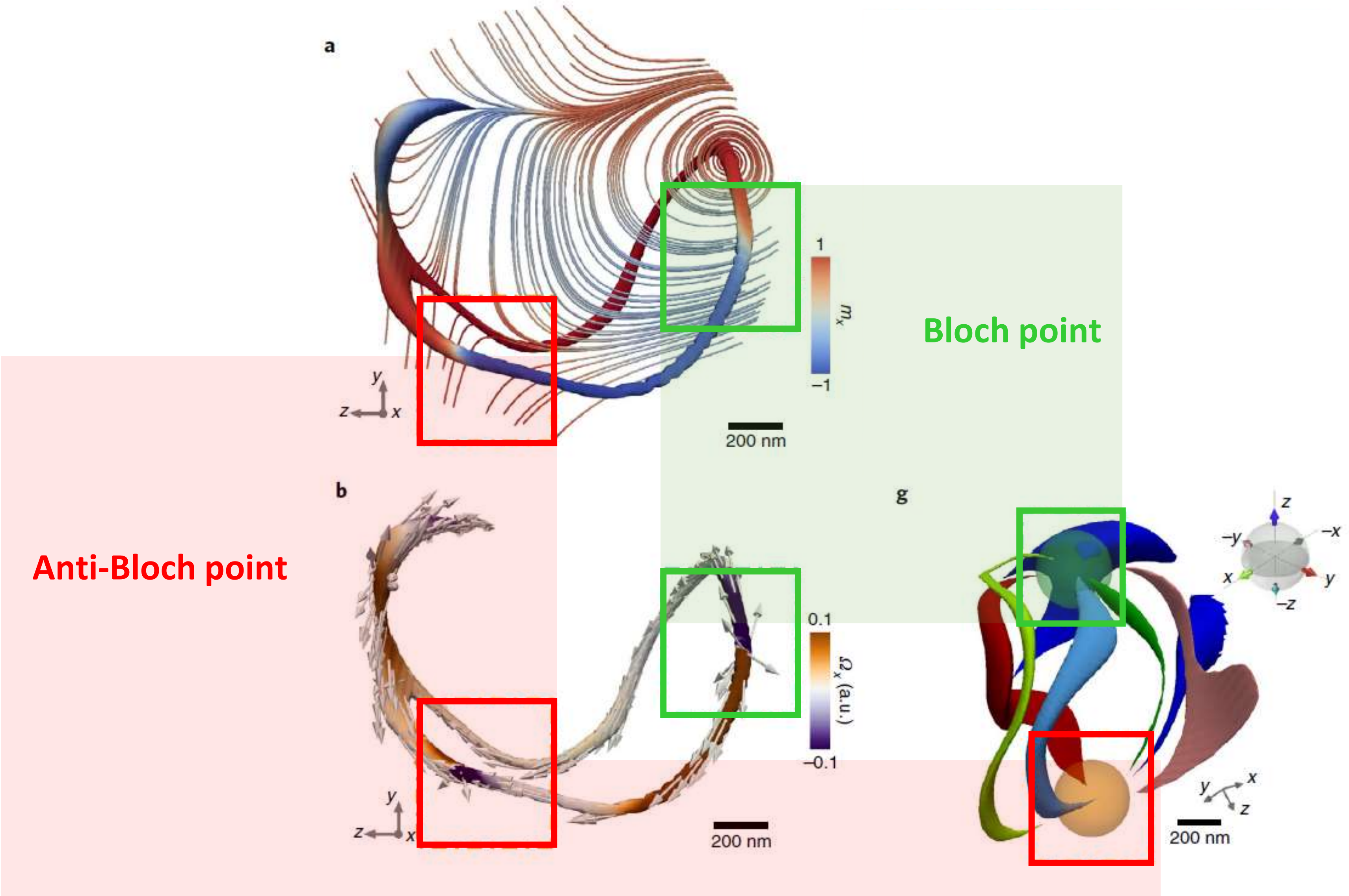

Results – stability of vorticity loops

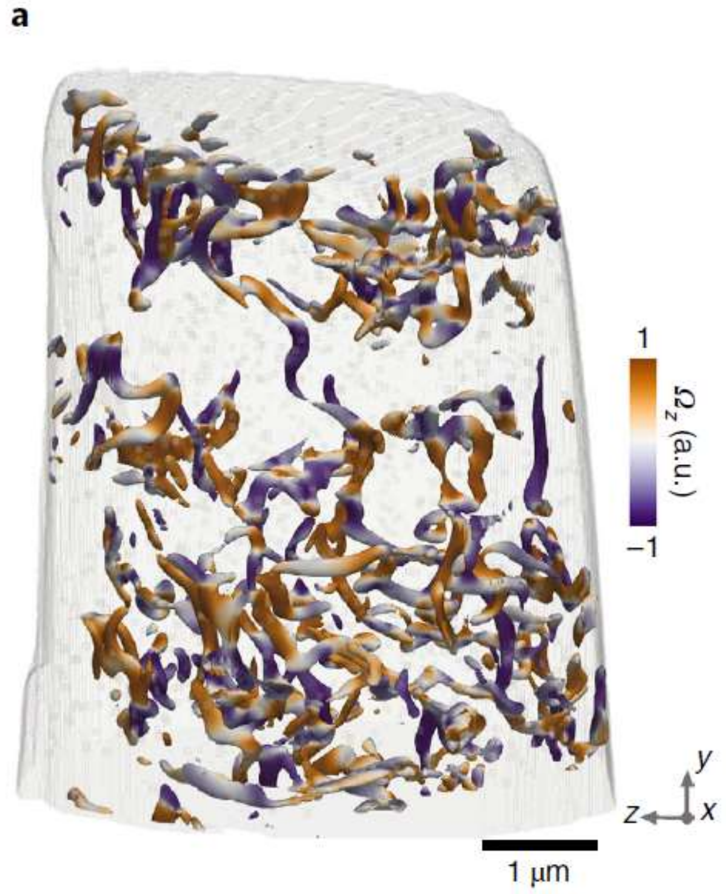

7 T magnetic field
along the long axis of the pillar
at **room temperature**

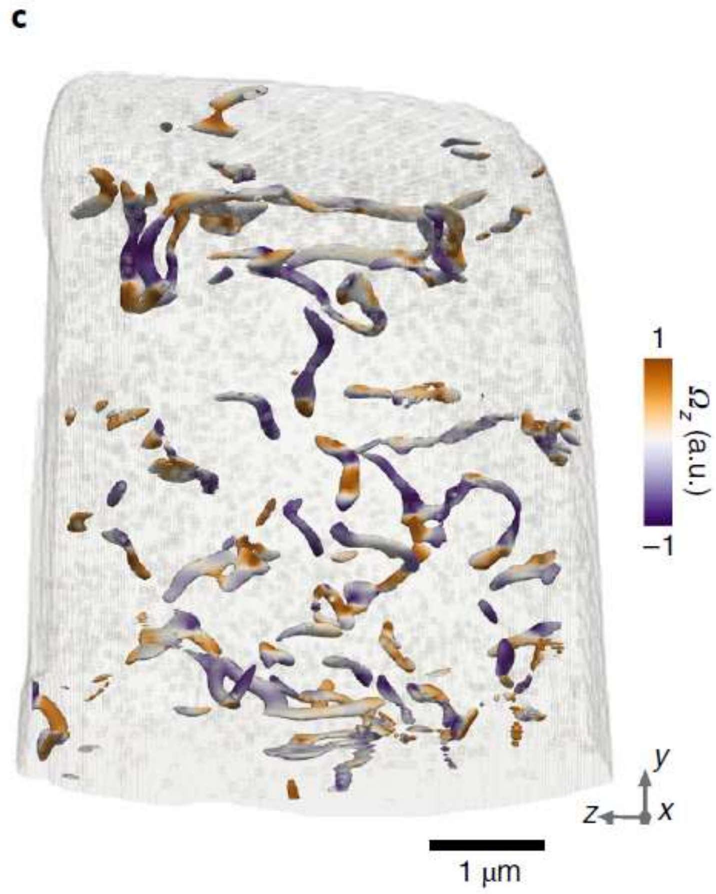

sample **heated to 400 K**
while applying
7 T magnetic field

→ no vortex loops after heating and magnetic field

→ vortex loops are metastable states

Outlook

X-ray magnetic laminography

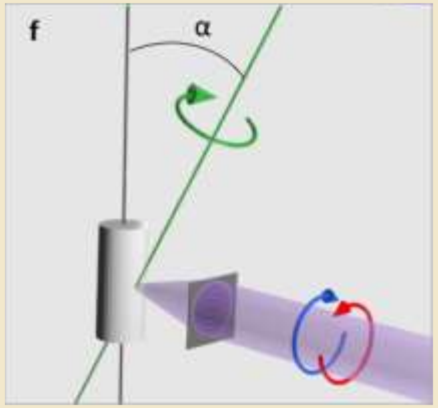

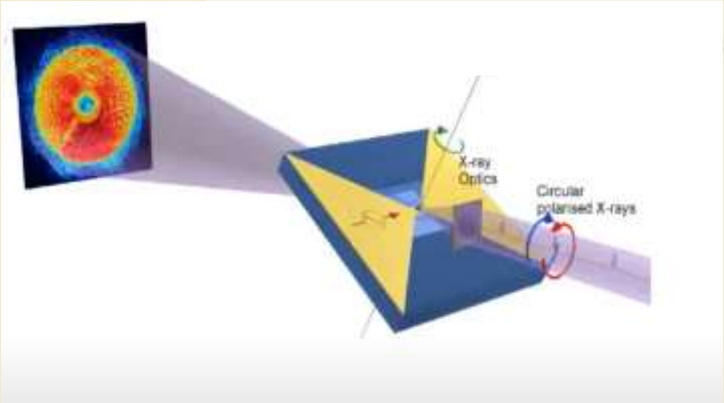

For 0° < α < 90°, **all three** components of the magnetization are measured with **one** rotation axis.

→ makes measurements simpler and sample set up much easier

→ 4th dimension

→ higher spatial resolution and sensitivity for nanoscale 3D structures

Single-step reconstruction

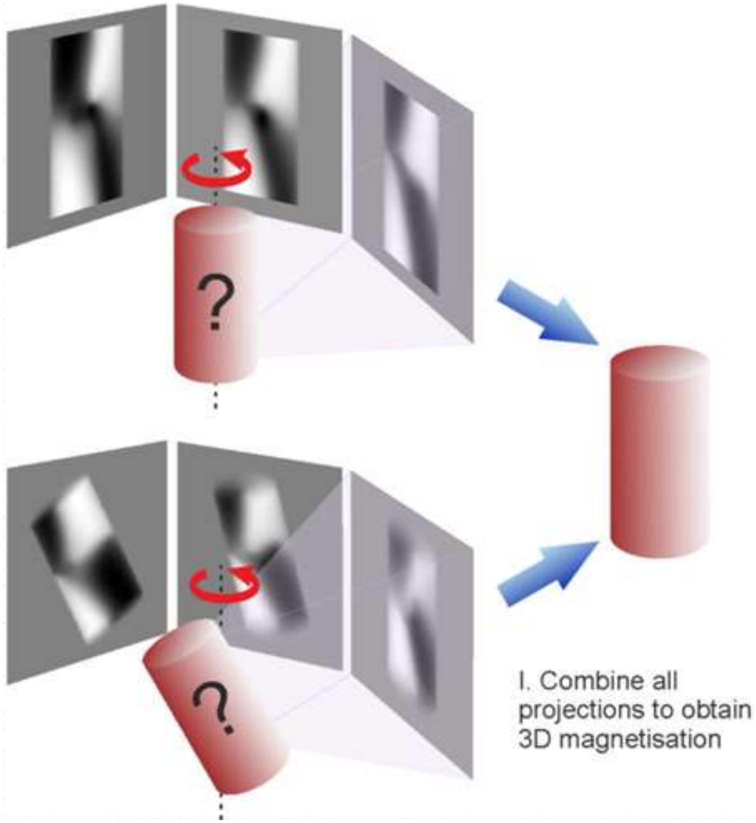

Thank you for your attention

References:

Slide 5:	Zang J., Cros V., Hoffmann A., Topology in Magnetism, Springer, p. 77 (2018)
	Donnelly C., Scagnoli V., Imaging three-dimensional magnetic systems with x-rays (2020)
Slide 10:	Donnelly C., Scagnoli V., et al., High-resolution hard x-ray magnetic imaging with dichroic ptychography (2016)
Slide 11:	Donnelly C., et al., Three-dimensional magnetization structures revealed with X-ray vector nanotomography (2017)
Slide 12:	Donnelly C., Scagnoli V., et al., High-resolution hard x-ray magnetic imaging with dichroic ptychography (2016)
Slide 15:	Donnelly C., et al., Tomographic reconstruction of a three-dimensional magnetization vector field (2018)
Slide 16:	Donnelly C., et al., Three-dimensional magnetization structures revealed with X-ray vector nanotomography (2017)
Slide 17:	Donnelly C., et al., Tomographic reconstruction of a three-dimensional magnetization vector field (2018)
Slide 18:	Donnelly C., et al., Tomographic reconstruction of a three-dimensional magnetization vector field (2018)
Slide 19:	Donnelly C., et al., Tomographic reconstruction of a three-dimensional magnetization vector field (2018)